RSC Advances

PAPER

View Article Online
View Journal | View Issue

Cite this: *RSC Adv.*, 2015, **5**, 17709

Amphiphilic porous polyhedral oligomeric silsesquioxanes (POSS) incorporated polyoxometalate-paired polymeric hybrids: interfacial catalysts for epoxidation reactions†

Yan Leng,*[a] Jiwei Zhao,[a] Pingping Jiang[a] and Jun Wang[b]

Received 24th December 2014
Accepted 5th February 2015

DOI: 10.1039/c4ra16956e

www.rsc.org/advances

A new strategy to fabricate amphiphilic polyoxometalate (POM)-paired polymeric hybrids *via* a free radical polymerization process using polyhedral oligomeric vinylsilsesquioxanes (POSS) and ionic liquids as the building block, followed by ion exchange was designed. The obtained hybrids were demonstrated to be porous materials with excellent amphiphilic properties, and can behave as efficient interfacial catalysts for the epoxidation of alkenes with H_2O_2 by stabilizing Pickering emulsions. The catalysts could be recovered by centrifugation and reused with no appreciable deactivation. The unique amphiphilic porous structure is revealed to be responsible for the catalysts' excellent performances in the epoxidation reaction by accelerating the mass transfer.

1. Introduction

The construction and exploration of amphiphilic structures is an area of growing research interest and technical importance in the design of advanced functional materials and devices.[1,2] In this context a variety of materials involving metal ions, biomaterials, and copolymers, have been constructed and explored for their potential applications in diverse fields.[3–5] Polyoxometalates (POMs) are a class of transition metal oxygen cluster and have been widely used as homogeneous catalysts for H_2O_2-based oxidation reactions.[6–9] Nevertheless, when (hydrophilic) aqueous H_2O_2 is used as the oxidant in organic transformations, one of the most troublesome problems is the insolubility of organic substances. Inspired by conventional amphiphiles, a number of amphiphilic POM catalytic systems have been reported, including phase transformation[10] and microemulsion formation.[11–13] However, most of these systems are homogeneous and suffer from poor catalyst recovery. Recently, the surface modification of metal oxide or silica matrix supported POM catalysts with hydrophilic and hydrophobic functional groups has proved to be an effective solution to form amphiphilic solid POM catalysts,[14,15] which can be utilized in heterogeneous catalysis, allowing facile separation and recycling after operation. However, this method still involves cumbersome and lengthy catalyst preparation procedures, and leaching of the active components. Therefore, a novel methodology for creating amphiphilic POM-based catalyst systems is needed.

Poly(ionic liquids) (PILs) resulting from the polymerization of ionic liquids (IL) monomers or copolymerization of ILs with other monomers are shown to constitute an interesting system to develop amphiphilic materials.[16,17] By varying the cations and/or anions with specific functions that constitute IL's structure, it is possible to design abundant PILs with required functionalities.[18,19] Indeed, POM-anions have been used as the counter anions for preparing "task-specific" ionic hybrids,[20,21] and several IL–POMs have been reported as efficient homogeneous, heterogeneous, or phase-separation catalysts for organic transformations.[22–25] In our recent work, an amphiphilic POM-paired PIL catalyst was prepared by employing the long chain alkyl imidazole ILs and carboxylic acid-functionalized imidazole ILs, and used as a highly efficient and recyclable heterogeneous catalyst in epoxidation of olefins with H_2O_2.[26,27]

Polyhedral oligomericsilsesquioxanes (POSS) are organic–inorganic molecules, with the general formula $R_8Si_8O_{12}$ where R is hydrogen or organic groups, such as alkyl, aryl or any of their derivatives.[28,29] Their unique star-shaped nanostructures and chemical properties, such as facile chemical modification, good pH tolerance, high temperature and oxidation resistance properties, make POSS an excellent building block for constructing multi-functional materials.[30–32] Taking into account that the incorporation of POSS into organic or inorganic polymer could create a micro/mesoporous matrix[33,34] and the fact that porous framework structure of the solid catalysts would

---

[a] The Key Laboratory of Food Colloids and Biotechnology, Ministry of Education, School of Chemical and Material Engineering, Jiangnan University, Wuxi 214122, China. E-mail: lengyan1114@126.com; Fax: +86-510-85917763; Tel: +86-510-85917090

[b] State Key Laboratory of Materials-Oriented Chemical Engineering, College of Chemistry and Chemical Engineering, Nanjing Tech University, Nanjing 210009, China

† Electronic supplementary information (ESI) available: Catalyst characterizations. See DOI: 10.1039/c4ra16956e

favor the increase of their catalytic performances because of benefits of structural stability and mass transfer, to construct POSS-containing porous POM-based PIL hybrids with more structural stability for application in H_2O_2-based oxidation catalysis is not only feasible but also profitable, and the multifunctional designability of polymeric IL cations can meet the requirement described above.

Herein, an innovative exploitation of POSS as building block for constructing porous POM-based polymeric hybrid catalysts (POSS–DIM_x–CIM_y–PW) with amphipathicity is proposed. POSS–DIM_x–CIM_y–PW are prepared by copolymerization of octavinyl POSS, dodecyl imidazole IL (DIM), and carboxylic acid-functionalized imidazole IL (CIM) without using any templates, followed by ion exchange with the $[PO_4(WO_3)_4]^{3-}$ species. The resulting catalysts are fully characterized by SEM, TEM, CHN elemental analysis, BET, contact angles (CA) tests, FT-IR, TG, and Raman (ESI†). Catalytic tests have shown that the POSS–DIM_x–CIM_y–PW exhibit extraordinary catalytic activities and recyclability in epoxidation of alkenes with H_2O_2.

2. Experimental section

2.1 Materials and methods

All chemicals were analytical grade and used as received. FT-IR spectra were recorded on a Nicolet 360 FT-IR instrument (KBr discs) in the 4000–400 cm^{-1} region. ^1H-NMR and ^{29}Si NMR spectra were measured with a Bruker DPX 400 spectrometer at ambient temperature in D_2O or $CDCl_3$ using 2,2-dimethyl-2-silapentane-5-sulfonate or TMS as internal reference. SEM image was performed on a HITACHI S-4800 field-emission scanning electron microscope. TG analysis was carried out with a STA409 instrument in dry air at a heating rate of 10 °C min^{-1}. TEM images were obtained with JEOL JEM-2100 electron microscope operated at 200 kV. The pore size distribution was derived from the desorption branch of N_2 isotherms using Barrett–Joyner–Halenda (BJH) method. Water repellency was checked by the contact angle of a pure water droplet using a contact angle meter of OCA 40. Elemental analyses (C, H, N) were performed on a CHN elemental analyzer (FlashEA 1112). The amount of leached tungsten species in the filtrate was measured using a Jarrell-Ash 1100 ICP-AES spectrometer.

2.2 Catalyst preparation

Preparation of IL monomers DIM and CIM. [3-Dodecyl-1-vinylimidazolium]Br (DIM): *N*-vinylimidazole (9.42 g, 0.10 mol) and bromododecane (25.0 g, 0.10 mol) were dissolved in ethanol (50 mL). Then, the mixture was stirred at 80 °C for 48 h under nitrogen atmosphere. On completion, the solvent was removed by distillation, and the solid product was washed with anhydrous acetone for three times to remove the unreacted substrates. After drying under vacuum, DIM was obtained. ^1H NMR (400 MHz, $CDCl_3$, TMS) δ (ppm) = 0.97 (s, 3H, $-CH_3$), 1.28 (m, 18H, $-CH_2$), 1.87 (m, 2H, $-CH_2$), 3.32 (m, 2H, $-CH_2$), 5.48 (d, 1H, –CH), 5.95 (d, 2H, $-CH_2$), 7.15 (d, 2H, –CH), 7.68 (d, 1H, –CH) (ESI, Fig. S1†).

[3-Propionic acid-1-vinylimidazolium]Br (CIM): *N*-vinylimidazole (9.42 g, 0.10 mol) and 3-bromopropionic acid (15.30 g, 0.10 mol) were dissolved in ethanol (50 mL). Then, the mixture was stirred at 80 °C for 24 h under nitrogen atmosphere. On completion, the white solid of CIM was obtained after the removing of solvent and washing with acetonitrile for three times. ^1H NMR (400 MHz, D_2O, TMS) for CIM δ (ppm) = 3.01 (t, 2H, $-CH_2$), 4.72 (t, 2H, $-CH_2$), 5.45 (d, 1H, –CH), 5.81 (d, 1H, –CH), 7.17 (m, 1H, –CH), 7.63 (s, 1H, –CH), 7.79 (s, 1H, –CH), 9.12 (s, 1H, –CH) (ESI, Fig. S2†).

Preparation of octavinyl POSS. Octavinyl POSS was prepared according to the previous literature.[35] Typically, in a 250 mL flask, vinyltriethoxysilane (19 g, 0.1 mol) was dissolved in 50 mL anhydrous ethanol. Then 10 mL hydrochloric acid and 8 mL deionized water were added into the above solution with vigorous stirring. The above reaction mixture was allowed to react for 48 h at room temperature. On completion, the white crystalline powder was filtered, washed with anhydrous ethanol, recrystallized in tetrahydrofuran/methanol (volume ratio: 1 : 3) mixture solvent and dried in vacuum at 80 °C for 10 h. ^{29}Si NMR (400 MHz, $CDCl_3$, TMS) δ (ppm) = 80.19 (ESI, Fig. S3†).

Preparation of POSS–DIM_x–CIM_y. POSS–DIM_x–CIM_y (x and y stands for the molar ratio of DIM with POSS and CIM with POSS, respectively) were synthesized through free radical polymerization of octavinyl POSS, DIM, and CIM. As a typical run for the synthesis of POSS–DIM_3–CIM_5, the obtained octavinyl POSS (0.63 g, 1 mmol), DIM (1.03 g, 3 mmol), CIM (1.24 g, 5 mmol), and azodiisobutyronitrile (AIBN, 0.06 g) were dissolved in a mixture solvent (1,4-dioxane 20 mL and methanol 20 mL). Then the solution was stirred at 75 °C for 24 h. After reaction, the above mixture was added dropwise into deionized water (100 mL) to afford the solid product. Elemental analysis, found: C: 45.32%, N: 7.93%, and H: 6.08%. Then the solid product POSS–DIM_x–CIM_y was filtered, washed with ethanol and dried under vacuum. The control polymers of POSS–DIM_8 and POSS–CIM_8 were prepared accordingly.

Preparation of POSS–DIM_x–CIM_y–PW. POM-paired ionic copolymer POSS–DIM_x–CIM_y–PW was prepared from the reaction between POSS–DIM_x–CIM_y and phosphotungstate ($H_3PO_4(WO_3)_4$, abbreviate as PW) in aqueous solution at room temperature for 2 h. The starting molar ratio of POSS–DIM_x–CIM_y to PW was 1 : $(x + y)/3$. Typically, a solution of H_3PO_4 (0.25 g, 2.5 mmol) in water (5 mL) was added to a solution of 2.5 g H_2WO_4 (10 mmol) in water (15 mL) and 30 wt% H_2O_2 (7 mL), the mixture was reacted for 30 min at room temperature with stirring. Then POSS–DIM_x–CIM_y (2.0 g) dissolved in anhydrous ethanol (20 mL) was added drop wise into the above solution. The mixture was stirred vigorously at room temperature for 2 h. The solid product POSS–DIM_3–CIM_5–PW was filtered, washed with small amount of water and ethanol, and dried. Elemental analysis, found: C: 25.76%, N: 4.59%, and H: 3.66%.

2.3 Catalytic tests

Cyclooctene (10 mmol), acetonitrile (10 mL), and catalyst (0.1 g, 0.035 mmol) were added into a 25 mL flask. Then 30 wt% H_2O_2 (12 mmol) was added into the solution at 70 °C within 10 min under vigorous stirring. After reaction, the reaction mixture was centrifuged to remove the solid catalyst, and the liquid was analyzed by a gas chromatography (GC). Other alkene substrates were tested accordingly. A five-run catalyst recycling was carried out for testing the reusability of catalyst. The catalyst was recovered by a centrifugation, washed with ethanol, and dried in vacuum.

3. Results and discussion

3.1 Catalyst preparation and characterization

The preparation of the POM-paired polymeric hybrids was carried out according to the procedures shown in Fig. 1. The IL monomers DIM and CIM were first prepared and characterized by ^{1}H NMR. The PIL POSS–DIM$_x$–CIM$_y$ was synthesized by the free radical copolymerization of octavinyl POSS, DIM and CIM using AIBN as the initiator. By varying the molar ratio of DIM and CIM to octavinyl POSS, a series of ionic copolymers POSS–DIM$_x$–CIM$_y$ could be prepared in the same way. The final catalyst POSS–DIM$_x$–CIM$_y$–PW was obtained by the anion-exchange of POSS–DIM$_x$–CIM$_y$ with the previously prepared $H_3[PO_4(WO_3)_4]$ in aqueous solution. Typically, the SEM image of POSS–DIM$_3$–CIM$_5$–PW shows the irregular coral-shaped morphology with micrometer size and nanoscale hollow structure (Fig. 2A). The TEM image in Fig. 2B confirms the amorphous nature of the polymeric hybrid POSS–DIM$_3$–CIM$_5$–PW. In the high-resolution TEM image, the observed dark nanoparticles with small size of about 1 nm indicate that the introduced PW has been uniformly dispersed in the PIL network. The TG patterns (Fig. 2C) for the POSS–DIM$_3$–CIM$_5$–PW shows a high thermal stability up to *ca.* 250 °C, which is higher than that of the conventional organic polymers. In addition, these obtained polymeric hybrids are insoluble in most common solvents, including water, acetonitrile, methanol, ethyl acetate, DMF, DMSO, and acetic acid at low temperatures, and thus can be used as the heterogeneous catalysts.

Fig. 2D illustrates the FT-IR spectra of polymeric hybrids POSS–DIM$_3$–CIM$_5$ and POSS–DIM$_3$–CIM$_5$–PW. The FT-IR spectrum of POSS–DIM$_3$–CIM$_5$ (Fig. 2D, curve a) clearly shows the band at 1113 cm^{-1} assigned to asymmetric vibration of Si–O–Si and the characteristic bands at 1740, 1570, and 2854–2930 cm^{-1} that are attributed to C=O, C=N, and CH$_2$ stretching vibrations, respectively, indicating the coexistence of POSS and IL units. After the combination of POSS–DIM$_3$–CIM$_5$ with $H_3[PO_4(WO_3)_4]$ (Fig. 2D, curve b), the peaks assigned to Si–O–Si and organic moiety in POSS–DIM$_3$–CIM$_5$–PW are consistent with those of the IR spectrum for individual POSS–DIM$_3$–CIM$_5$. Moreover, characteristic vibration bands for the $[PO_4(WO_3)_4]^{3-}$ species are observed for POSS–DIM$_3$–CIM$_5$–PW at 1080, 951, 883 and 820 cm^{-1}, assignable to vibrations of P–O$_a$, W=O$_d$, W–O$_b$–W and W–O$_c$–W, respectively, which are in reasonable agreement with those of the IR spectra for $[PO_4(WO_3)_4]^{3-}$ in previous literatures.[10,36–39] Additionally, the Raman spectrum of POSS–DIM$_3$–CIM$_5$–PW (ESI, Fig. S6†) shows the characteristic bands at 951, 989, and 1007 cm^{-1} for tungstate polyoxoanion vibrations,[40] which further confirms the structure of $[PO_4(WO_3)_4]^{3-}$ anion.

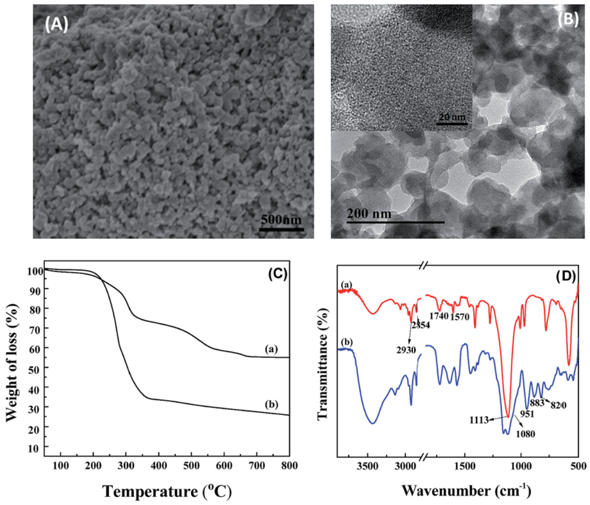

Fig. 2 (A) SEM image of POSS–DIM$_3$–CIM$_5$–PW; (B) TEM image of POSS–DIM$_3$–CIM$_5$–PW; (C) TG curves of (a) POSS–DIM$_3$–CIM$_5$–PW and (b) POSS–DIM$_3$–CIM$_5$; (D) FT-IR spectra of (a) POSS–DIM$_3$–CIM$_8$ and (b) POSS–DIM$_3$–CIM$_5$–PW.

Fig. 3A and B show the N_2 adsorption–desorption isotherms and the corresponding pore size distributions of the prepared polymeric hybrids, respectively. The POSS-free polymeric hybrid DIM$_3$–CIM$_5$–PW is a nonporous material with a surface area of only 6.2 cm^2 g^{-1} (curve e in Fig. 3A and B, Table 1, entry 5). For the POSS-containing polymeric hybrids POSS–DIM$_x$–CIM$_y$–PW, all the samples display a typical IV type isotherm, giving a steep increase at a relative pressure of $0.8 < P/P_0 < 1$, indicating the presence of porous structures, including mesopores and macropores. This demonstrates that the POSS plays an important role in the pore formation. The optimum specific surface 24.2 cm^2 g^{-1} and pore volume 0.175 cm^3 g^{-1} are obtained when the

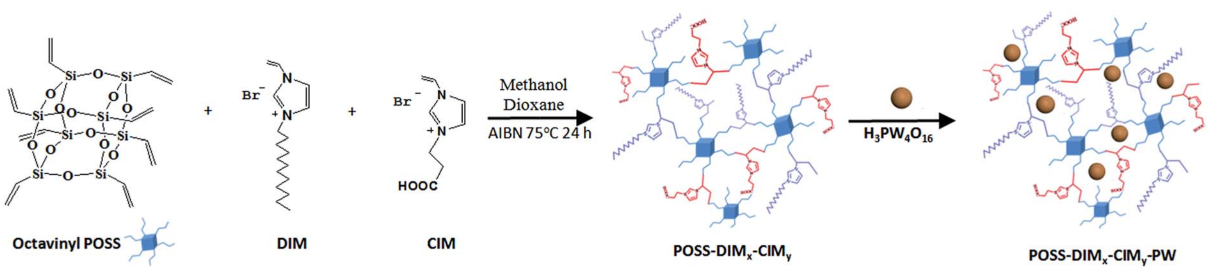

Fig. 1 Schematic illustration outlining the preparation and structure of the catalyst POSS–DIM$_x$–CIM$_y$–PW.

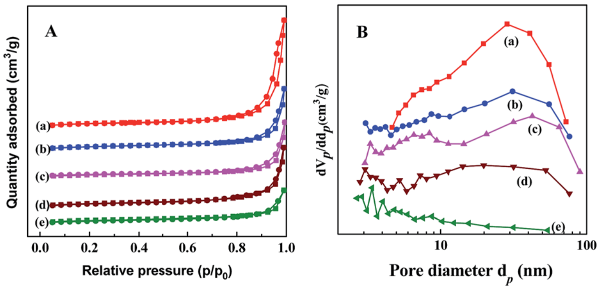

Fig. 3 (A) Nitrogen adsorption–desorption isotherms and (B) BJH pore size distributions of (a) POSS–DIM$_3$–CIM$_5$–PW, (b) POSS–DIM$_5$–CIM$_5$–PW, (c) POSS–DIM$_5$–CIM$_3$–PW, (d) POSS–DIM$_8$–CIM$_6$–PW, (e) DIM$_3$–CIM$_5$–PW.

mole ratio of DIM to CIM is 3 : 5 (Table 1, entry 1). The higher molar ratio of DIM to CIM leads to less porous systems, most probably due to the blockage of channel by long chain dodecyl in DIM.

The combination of the hydrophilic CIM with hydrophobic DIM into a single POSS-containing polymeric hybrid structure could generate unique amphiphilic property in principle. To understand the wettability of these hybrids POSS–DIM$_x$–CIM$_y$–PW, we carried out the CA tests. As can be seen in Fig. 4A, when a water droplet is brought in contact with the surface of the samples, it yields a CA of 62.8° on the surface of POSS–DIM$_3$–CIM$_5$–PW, implying its hydrophilicity. The CAs increased from 62.8° to 105.8° as the molar ratio of DIM to CIM increased, the enhanced hydrophobicity is attributable to the surface chemistry change due to the increasing of hydrophobic DIM in the hybrid catalysts. With cyclooctene as the testing droplet, the CAs were measured to be less than 5° for all samples (Fig. 4B), demonstrating excellent surface lipophilicity. Therefore, the above results indicate that the unique amphiphilic PW-paired polymeric hybrids could be obtained through tuning the content of DIM and CIM in POSS–DIM$_x$–CIM$_y$–PW.

3.2 Catalytic activity in the epoxidation reaction

The catalytic activity of the POSS–DIM$_3$–CIM$_5$–PW was tested in the epoxidation of cyclooctene using H_2O_2 in various solvents over the reaction times of 1 h, 2 h, and 4 h, respectively (Fig. 5). During the reaction process, the catalyst POSS–DIM$_3$–CIM$_5$–PW was insoluble in all cases, and exhibited different catalytic activities with satisfying selectivity above 99%. In the acetonitrile and acetic acid solvents, excellent conversions (≥99%) were observed in a short reaction time of 1 h. It is noteworthy that peroxyacids generated from the oxidation of carboxylic acid with H_2O_2 in acetic acid solvent may take part in the epoxidation. In order to confirm this, a control experiment without the addition of catalyst was performed, and a conversion of 84.4% with 95% selectivity was obtained in the reaction time of 4 h. When the catalyst was added, the reaction rate significantly increased, the reaction proceeded well and completed within only 15 min. For ethanol and methanol solvents, high conversions were also obtained by prolonging the reaction time to 4 h. When ethyl acetate and dichloroethane were used as a solvent, a liquid–liquid biphasic reaction system was formed due to the immiscibility of these solvents with aqueous H_2O_2. After the addition of POSS–DIM$_3$–CIM$_5$–PW, the catalyst tends to migrate toward the oil/aqueous interface due to their amphiphilic feature (Fig. 6a), and stable emulsions were formed after stirring (Fig. 6b). The optical microscopy image of the emulsion (Fig. 6c) shows droplet sizes in the range of 5–10 μm. After the reaction, the solid catalyst can be separated by centrifugation and recycled in the next run. The phenomenon observed here is very similar to that of the Pickering Interfacial Catalysis,[41,42] that the amphiphilic catalysts localized at the interface of both phases can stabilize emulsions, allowing facile separation and recycling. Herein, the formation of the Pickering emulsion enhances the contact region, the substrates cyclooctene and H_2O_2 molecules could infiltrate into the amphiphilic catalyst effectively (Fig. 6d). Thus, with ethyl acetate and dichloroethane as the solvent, very high conversions (>98%) were obtained as well.

Considering that the chlorocarbons have environment safety problems such as high toxicity and carcinogenicity. Moreover, the epoxidation process using acetic acid and H_2O_2 may cause severe safety and corrosion problems relative to the peroxyacids. Therefore, acetonitrile and ethyl acetate were selected as the

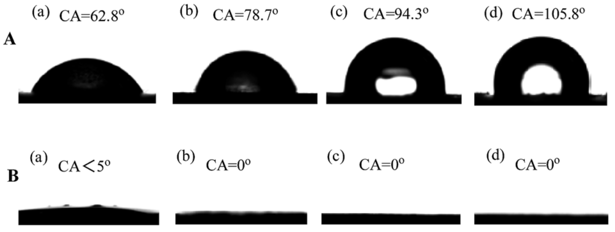

Fig. 4 (A) Water droplets and (B) cyclooctene droplets on the surface of catalysts (a) POSS–DIM$_3$–CIM$_5$–PW, (b) POSS–DIM$_5$–CIM$_5$–PW, (c) POSS–DIM$_5$–CIM$_3$–PW, and (d) POSS–DIM$_8$–CIM$_6$–PW.

Table 1 The textural parameters of POSS–DIM$_x$–CIM$_y$–PW catalysts

Entry	Samples	S_{BET}^{a} (m^2 g^{-1})	V_p^{b} (cm^3 g^{-1})	D_{av}^{c} (nm)
1	POSS–DIM$_3$–CIM$_5$–PW	24.2	0.175	30.3
2	POSS–DIM$_5$–CIM$_5$–PW	18.6	0.11	28.6
3	POSS–DIM$_5$–CIM$_3$–PW	18.8	0.113	29.4
4	POSS–DIM$_8$–CIM$_6$–PW	12.9	0.101	24.3
5	DIM$_3$–CIM$_5$–PW	6.2	0.062	15.2

[a] BET surface area. [b] Total pore volume. [c] Average pore diameter.

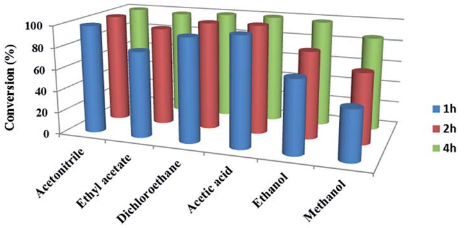

Fig. 5 Catalytic activities of POSS–DIM_3–CIM_5–PW in epoxidation of cyclooctene with H_2O_2 in different solvents.[a] Reaction conditions: catalyst (0.1 g), cyclooctene (10 mmol), 30% H_2O_2 (12 mmol), solvent (10 mL), 70 °C.

Table 2 Catalytic performances of various catalysts for the epoxidation of cyclooctene with H_2O_2[a]

		Acetonitrile		Ethyl acetate	
Entry	Catalyst	Con[b] (%)	Sel[c] (%)	Con[b] (%)	Sel[c] (%)
1	POSS–DIM_3–CIM_5	7	100	4	100
2	POSS–DIM_8–PW	63	100	67	100
3	POSS–CIM_8–PW	68	100	18	100
4	POSS–DIM_3–CIM_5–PW	100	100	98	100

[a] Reaction conditions: 0.1 g catalyst, 10 mmol cyclooctene, 12 mmol H_2O_2 (30%), 10 mL solvent, 70 °C, 4 h. [b] Conversion of the substrate. [c] Selectivity for the epoxide product.

solvent for the following catalytic investigation. The catalytic activities of various control catalysts were assessed in comparison to POSS–DIM_3–CIM_5–PW for epoxidation of cyclooctene with H_2O_2. The results are shown in Table 2, it can be seen that the POSS containing hybrids are all insoluble in the reaction system, and caused heterogeneous catalysis. However, the PW-free polymer POSS–DIM_3–CIM_5 shows very low activities (Table 2, entry 1), and CIM-free POSS–DIM_8–PW and DIM-free POSS–CIM_8–PW (Table 2, entries 2 and 3) affords much lower conversions than that POSS–DIM_3–CIM_5–PW did in both acetonitrile and ethyl acetate solvents. It appears that the low catalytic activities of POSS–DIM_8–PW and POSS–CIM_8–PW are mostly due to the poor interfacial interaction, since the systems using ethyl acetate as the solvent could hardly form an emulsion. Therefore, all the above comparisons suggest that the coexistence of DIM and CIM unites in polymeric cations endows the hybrid catalyst with unique amphiphilic feature, and plays an important role for the emulsion catalytic system, which account for the excellent catalytic performance.

To illustrate the influence of the content of DIM and CIM on the catalytic activity of hybrid catalysts, we also tested the catalytic kinetics of POSS–DIM_x–CIM_y–PW for the epoxidation of cyclooctene in acetonitrile and ethyl acetate, respectively (Fig. 7). Pickering emulsions taking place in all cases, and very high conversions are observed over these polymeric catalysts with a reaction time of about 3 h. However, the reaction rates of POSS–DIM_x–CIM_y–PW gradually decreased as the molar ratio of DIM to CIM increased. This variation was also reflected in their pore structure as suggested by Nitrogen adsorption–desorption characterization. It is thus propose that the catalytic activity of POSS–DIM_x–CIM_y–PW is reasonably related to its porous structure, and the comparatively high surface area and large pore volume favor higher catalytic rate.

In order to investigate the scope of the amphiphilic porous catalyst for epoxidation reactions, the substrates such as cyclohexene, 1-octene, 1-hexene, *cis*-3-hexenol, and bipentene were also investigated on the catalyst POSS–DIM_3–CIM_5–PW, with the results shown in Table 3. It can be seen that the present catalyst POSS-DIM_3–CIM_5–PW could be applied to the epoxidation of various alkenes using H_2O_2, and good to excellent activities and selectivity were obtained.

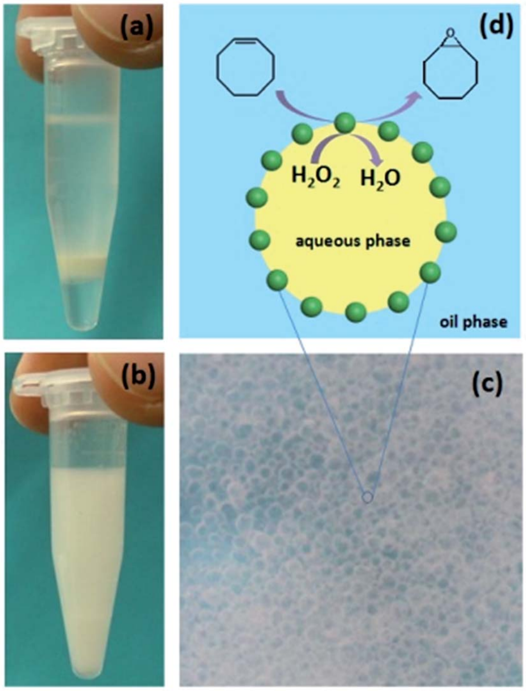

Fig. 6 (a) Photograph of POSS–DIM_3–CIM_5–PW appeared at the H_2O_2/(cyclooctene + ethyl acetate) interface; (b) photograph of the reaction system after stirring for 10 min; (c) optical micrograph of the emulsions; (d) scheme of amphiphilic catalysts located at the H_2O_2/(cyclooctene + ethyl acetate) interface for the epoxidation of cyclooctene with H_2O_2.

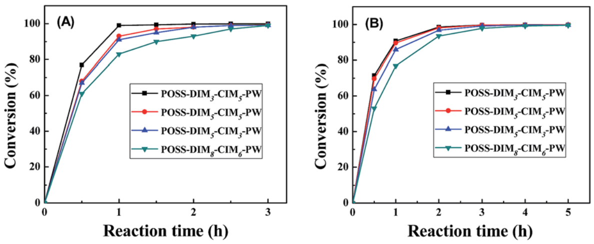

Fig. 7 Time profile of epoxidation of cyclooctene catalyzed by different catalysts in (A) acetonitrile and (B) ethyl acetate solvents. Reaction conditions: 0.1 g catalyst, 10 mmol cyclooctene, 12 mmol H_2O_2 (30%), 10 mL solvent, 70 °C.

Table 3 Epoxidation of various alkenes with H_2O_2 catalyzed by POSS–DIM$_3$–CIM$_5$–PW[a]

Entry	Substrate	Reaction time (h)	Con[b] (%)	Sel[c] (%)
1	Cyclooctene	1	99	100
2	Cyclohexene	3	98	95
3	1-Octene	6	56	100
4	1-Hexene	4	49	100
5	*cis*-3-Hexenol	4	99	94
6	Bipentene	4	86	98

[a] Reaction conditions: catalyst (0.1 g), substrate (10 mmol), 30% H_2O_2 (12 mmol), acetonitrile (10 mL), 70 °C. [b] Conversion of the substrate. [c] Selectivity for the epoxide product. Byproducts for entry 2: 2-cyclohexen-1-ol (0.93 mmol) and 2-cyclohexen-1-one (0.51 mmol); entry 3: octylaldehyde; entry 4: 2-hexenone; entry 5: 3,4-epoxyhexane-1-aldehyde; entry 6: 1,2:8,9-diepoxy-*p*-menthane and 1,2-ene-*p*-menth-8,9-epoxy.

3.3 Catalyst reusability

Finally, the reusability of amphiphilic porous catalyst was evaluated on the epoxidation of cyclooctene over POSS–DIM$_3$–CIM$_5$–PW. After each cycle, the catalyst was separated from the reaction system by centrifugation, washed with ethanol, and dried at 80 °C. As shown in Fig. 8, the five-run test gave 100% selectivity without significant loss of conversion. It is explicitly more stable than our previous prepared POSS-free polymeric POM hybrid.[27] The IR spectrum for the recovered POSS–DIM$_3$–CIM$_5$–PW in Fig. 9 was well consistent with that of the fresh one, revealing a durable catalyst structure. However, the intensities of the IR bands for the PW decreased lightly. Moreover, the results of ICP-AES analysis for the reacted filtrate showed that about 3.1 wt% W in the catalyst has been leached into the reaction media in the first run, but in the followed runs, the leaching amounts were negligible. It is thus supposed that there is a small amount of PW in the fresh catalyst that only losely interacts with polymeric cations tends to leach into the liquid phase in the first reaction run. The above result implies that the featured three dimensional network framework of POSS–DIM$_3$–CIM$_5$–PW derived from POSS units endows the catalyst with excellent structural stability, and accounts for the steadily catalytic reuse.

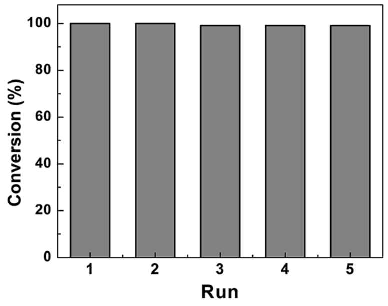

Fig. 8 Catalytic reusability of POSS–DIM$_3$–CIM$_5$–PW for the epoxidation of cyclooctene with H_2O_2. Reaction conditions: catalyst (0.1 g), cyclooctene (10 mmol), 30% H_2O_2 (12 mmol), acetonitrile (10 mL), 70 °C, 2 h.

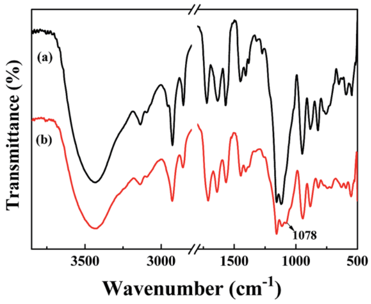

Fig. 9 FTIR spectra of (a) fresh POSS–DIM$_3$–CIM$_5$–PW and (b) recycled POSS–DIM$_3$–CIM$_5$–PW.

4. Conclusion

In summary, we have demonstrated the successful application of octavinyl POSS and IL as building blocks for constructing amphiphilic porous POM-paired ionic hybrids POSS–DIM$_x$–CIM$_y$–PW *via* free radical polymerization and ion exchange reaction. The obtained hybrids were found to be highly efficient interfacial catalysts for epoxidation of alkenes with H_2O_2 as oxidant. The catalyst was recovered easily and reused for five runs without observing loss in catalytic activity. The overall superior catalytic activity, high selectivity and excellent recyclability of POSS–DIM$_3$–CIM$_5$–PW as a heterogeneous catalyst could be attributed to its amphiphilic surface and pore structure, which allow for a rapid diffusion of the reactants into the reactive PW centers.

Acknowledgements

The authors thank the National Natural Science Foundation of China (no. 21206052 and 21136005), the Opening Foundation of the State Key Laboratory of Materials-Oriented Chemical Engineering (no. KL13-09), and MOE & SAFEA for the 111 Project (no. B13025).

Notes and references

1 T. Chen, S. Xu, T. Zhao, L. Zhu, D. Wei, Y. Li, H. Zhang and C. Zhao, *ACS Appl. Mater. Interfaces*, 2012, **4**, 5766–5774.
2 W. Cao and L. Zhu, *Macromolecules*, 2011, **44**, 1500–1512.
3 B. S. Souza, E. C. Leopoldino, D. W. Tondo, J. Dupont and F. Nome, *Langmuir*, 2012, **28**, 833–840.
4 J. Hu, T. Wu, G. Zhang and S. Liu, *J. Am. Chem. Soc.*, 2012, **134**, 7624–7627.
5 Y. M. A. Yamada, S. M. Sarkar and Y. Uozumi, *J. Am. Chem. Soc.*, 2012, **134**, 9285–9290.
6 Y. Song and R. Tsunashima, *Chem. Soc. Rev.*, 2012, **41**, 7384–7402.
7 H. Lv, Y. V. Geletii, C. Zhao, J. W. Vickers, G. Zhu, Z. Luo, J. Song, T. Lian, D. G. Musaev and C. L. Hill, *Chem. Soc. Rev.*, 2012, **41**, 7572–7589.
8 Y. Zhou, G. Chen, Z. Long and J. Wang, *RSC Adv.*, 2014, **4**, 42092–42113.

9 N. Mizuno, K. Yamaguchi and K. Kamata, *Coord. Chem. Rev.*, 2005, **249**, 1944–1956.

10 Z. Xi, N. Zhou, Y. Sun and K. Li, *Science*, 2001, **292**, 1139–1141.

11 J. Xu, S. Zhao, Y. Ji and Y. Song, *Chem.–Eur. J.*, 2013, **19**, 709–715.

12 J. Gao, Y. Zhang, G. Jia, Z. Jiang, S. Wang, H. Lu, B. Song and C. Li, *Chem. Commun.*, 2008, 332–334.

13 P. Yin, J. Wang, Z. Xiao, P. Wu, Y. Wei and T. Liu, *Chem.–Eur. J.*, 2012, **18**, 9174–9178.

14 K. Inumaru, T. Ishihara, Y. Kamiya, T. Okuhara and S. Yamanaka, *Angew. Chem., Int. Ed.*, 2007, **46**, 7625–7628.

15 F. Su, L. Ma, Y. Guo and W. Li, *Catal. Sci. Technol.*, 2012, **2**, 2367–2374.

16 Y. M. A. Yamada, S. M. Sarkar and Y. Uozumi, *J. Am. Chem. Soc.*, 2012, **134**, 9285–9290.

17 D. Mecerreyes, *Prog. Polym. Sci.*, 2011, **36**, 1629–1648.

18 D. Chaturvedi, *Curr. Org. Chem.*, 2011, **15**, 1236–1248.

19 N. R. Sahraie, J. P. Paraknowitsch, C. Göbel, A. Thomas and P. Strasser, *J. Am. Chem. Soc.*, 2014, **136**, 14486–14497.

20 R. N. Biboum, F. Doungmene, B. Keita, P. Oliveira, L. Nadjo, B. Lepoittevin, P. Roger, F. Brisset, P. Mialane, A. Dolbecq, I. M. Mbomekalle, C. Pichon, P. Yin, T. Liu and R. Contant, *J. Mater. Chem.*, 2012, **22**, 319–323.

21 S. Doherty, J. G. Knight, J. R. Ellison, D. Weekes, R. W. Harrington, C. Hardacre and H. Manyar, *Green Chem.*, 2012, **14**, 925–929.

22 Y. Leng, J. Wang, D. Zhu, X. Ren, H. Ge and L. Shen, *Angew. Chem., Int. Ed.*, 2009, **48**, 168–171.

23 S. Doherty, J. G. Knight, J. R. Ellison, D. Weekes, R. W. Harrington, C. Hardacre and H. Manyar, *Green Chem.*, 2012, **14**, 925–929.

24 G. Chen, Y. Zhou, P. Zhao, Z. Long and J. Wang, *ChemPlusChem*, 2013, **78**, 561–569.

25 P. Zhao, J. Wang, G. Chen, Y. Chen and J. Huang, *Catal. Sci. Technol.*, 2013, **3**, 1394–1404.

26 Y. Leng, J. Zhao, P. Jiang and J. Wang, *ACS Appl. Mater. Interfaces*, 2014, **6**, 5947–5954.

27 Y. Leng, J. Wu, P. Jiang and J. Wang, *Catal. Sci. Technol.*, 2014, **4**, 1293–1300.

28 K. Tanaka, F. Ishiguro and Y. Chujo, *J. Am. Chem. Soc.*, 2010, **132**, 17649–17651.

29 M. C. Kung, M. V. Riofski, M. N. Missaghi and H. H. Kung, *Chem. Commun.*, 2014, **50**, 3262–3276.

30 J. Han, Y. Zheng, S. Zheng, S. Li, T. Hu, A. Tang and C. Gao, *Chem. Commun.*, 2014, **50**, 8712–8714.

31 Z. Ruan, W. Rong, X. Zhan, Q. Li and Z. Li, *Polym. Chem.*, 2014, **5**, 5994–6002.

32 K. Tanaka and Y. Chujo, *J. Mater. Chem.*, 2012, **22**, 1733–1746.

33 M. Seino, W. Wang, J. E. Lofgreen, D. P. Puzzo, T. Manabe and G. A. Ozin, *J. Am. Chem. Soc.*, 2011, **133**, 18082–18085.

34 H. Lin, J. Ou, Z. Zhang, J. Dong and H. Zou, *Chem. Commun.*, 2013, **49**, 231–233.

35 H. He, B. Li, J. Dong, Y. Lei, T. Wang, Q. Yu, Y. Feng and Y. Sun, *ACS Appl. Mater. Interfaces*, 2013, **5**, 8058–8066.

36 J. Gao, Y. Chen, B. Han, Z. Feng, C. Li, N. Zhou, S. Gao and Z. Xi, *J. Mol. Catal. A: Chem.*, 2004, **210**, 197–204.

37 J. Li, S. Gao, M. Li, R. Zhang and Z. Xi, *J. Mol. Catal. A: Chem.*, 2004, **218**, 247–252.

38 Y. Sun, Z. Xi and G. Cao, *J. Mol. Catal. A: Chem.*, 2001, **166**, 219–224.

39 S. Zhang, S. Gao, Z. Xi and J. Xu, *Catal. Commun.*, 2007, **8**, 531–534.

40 E. P. Ferreira-Neto, S. Ullah, F. L. S. de Carvalho, A. L. de Souza, M. de Oliveira Jr, J. F. Schneider, Y. P. Mascarenhas, A. M. Jorge Jr and U. P. Rodrigues-Filho, *Mater. Chem. Phys.*, 2015, **153**, 410–421.

41 W. Zhou, L. Fang, Z. Fan, B. Albela, L. Bonneviot, F. De Campo, M. Pera-Titus and J. Clacens, *J. Am. Chem. Soc.*, 2014, **136**, 4869–4872.

42 H. Tan, P. Zhang, L. Wang, D. Yang and K. Zhou, *Chem. Commun.*, 2011, **47**, 11903–11905.